Journal of Advanced Ceramics
2022, **11**(11): 1687–1695
https://doi.org/10.1007/s40145-022-0640-0
ISSN 2226-4108
CN 10-1154/TQ
Research Article

Self-healing behavior of Ti_2AlC at a low oxygen partial pressure

Boxiang YAO[a], Shibo LI[a,*], Weiwei ZHANG[a], Wenbo YU[a], Yang ZHOU[a], Shukai FAN[b], Guoping BEI[b]

[a]*Center of Materials Science and Engineering, School of Mechanical, Electronic and Control Engineering, Beijing Jiaotong University, Beijing 100044, China*
[b]*China Porcelain Fuchi (Suzhou) High Tech Nano Materials Co., Ltd., Suzhou 215100, China*

Received: May 27, 2022; Revised: July 26, 2022; Accepted: August 10, 2022

Abstract: Ti_2AlC, a MAX phase ceramic, has an attractive self-healing ability to restore performance via the oxidation-induced crack healing mechanism upon healing at high temperatures in air (high oxygen partial pressures). However, such healing ability to repair damages in vacuum or low oxygen partial pressure conditions remains unknown. Here, we report on the self-healing behavior of Ti_2AlC at a low oxygen partial pressure of about 1 Pa. The experimental results showed that the strength recovery depends on both healing temperature and time. After healing at 1400 ℃ for 1–4 h, the healed samples exhibited the recovered strengths even exceeding the original strength of 375 MPa. The maximum recovered strength of ~422 MPa was achieved in the healed Ti_2AlC sample after healing at 1400 ℃ for 4 h, about 13% higher than the original strength. Damages were healed by the formed TiC_x from the decomposition of Ti_2AlC. The decomposition-induced crack healing as a new mechanism in the low oxygen partial pressure condition was disclosed for the MAX ceramics. The present study illustrates that key components made of Ti_2AlC can prolong their service life and keep their reliability during use at high temperatures in low oxygen partial pressures.

Keywords: MAX ceramics; Ti_2AlC; self-healing; low oxygen partial pressures; strength recovery; mechanism

1 Introduction

Advanced ceramic materials are widely used in high-temperature environments due to their attractive stability, high strength, and oxidation resistance at high temperatures. However, the intrinsic brittleness of ceramics makes them sensitive to the presence of surface cracks, resulting in a loss in performance or even a sudden catastrophic failure during service [1]. One of the effective methods to overcome brittleness is the healing of cracks as they appear. Therefore, research has been carried out for over fifty years on the crack healing behavior of the ceramics including oxides (ZnO, UO_2, Al_2O_3, etc.), carbides (SiC, ZrC, etc.), nitrides (Si_3N_4, TiN, etc.), and MAX phases as well as their composites [2–13]. Generally, the oxidation-induced crack healing is the main mechanism for binary carbides and nitrides, and ternary MAX phases upon healing at high temperatures in air with high oxygen partial pressures. The cracks in such materials are partly or completely filled by oxides formed through oxidation.

Among them, MAX phase ceramics (where M refers

* Corresponding author.
E-mail: shbli1@bjtu.edu.cn

to an element of the transition metal, A is an element of group IIIA or IVA, and X is C or N [14]) exhibit attractive crack healing performance at relatively low temperatures and short time [1,12,13,15–19]. For example, Ti_3AlC_2 can completely heal a crack with a length of 7 mm and a width of 5 μm after healing at 1100 ℃ in air for 2 h [15]. The main healing mechanism for Ti_3AlC_2 is the filling of cracks with Al_2O_3 and TiO_2. Ti_2AlC has an ability to repeatedly heal introduced cracks with a size of ~2 mm at a given location at 1200 ℃ for 2 h in air. Such cracks were filled by the formation of Al_2O_3 and TiO_2 [1]. A fine-grained Cr_2AlC (~2 μm) MAX ceramic also demonstrates an ability to restore the flexural strength through the filling of cracks with only Al_2O_3 at 1100 ℃ in air for 4 h [16]. Moreover, Ti_2SnC can heal thermal-shock-induced cracks at a relatively low temperature of 800 ℃ within 1 h in air, leading to the recovery of electrical conductivity and flexural strength [17]. Healing is accomplished by the formation of TiO_2 and SnO_2 oxides at the site of damage.

Based on the above discussions, it is known that the crack healing mechanism driven by oxidation is efficient in air. However, high-temperature structural components made of such ceramics applied in hypersonic vehicles during flight, gas turbines under combustion, and industrial vacuum furnaces during work are generally exposed to low oxygen partial pressures. Cracks in the components will not be completely healed by the formation of oxides due to the suppression of the formation of the oxides in Mo–Si–B alloys [20] or the evaporation of the oxides in SiC and its composites [21–23] under low oxygen partial pressure conditions.

So far, most investigations have focused on the oxidation-induced crack healing behavior of the MAX ceramics in air. Work on the crack healing of MAX at low oxygen partial pressures has been much less focused. Only Ti_2SnC was reported that it can heal quenching-induced cracks at 800 ℃ for 1 h at a low oxygen partial pressure of 5 Pa [24]. Elemental Sn precipitates from the structure of Ti_2SnC and fills cracks. Therefore, Sn-precipitation-induced crack healing in Ti_2SnC leads to the complete recovery of the electrical conductivity at low oxygen partial pressures [24]. In the MAX family, Ti_2AlC is expected to be an attractive candidate for high-temperature applications in the gas turbines under combustion, heat elements and liners for industrial vacuum furnaces, and nozzles due to its good oxidation resistance [25–27], exceptional ablation resistance [28], and nonsusceptibility to thermal shock [29]. Such high-temperature components made of Ti_2AlC generally work under low oxygen partial pressure conditions, while whether Ti_2AlC can repair damages to prolong their service life is unknown. Therefore, it is necessary to investigate and understand the crack healing behavior of Ti_2AlC under low oxygen partial pressure conditions.

In the present study, the self-healing behavior of Ti_2AlC at a low oxygen partial pressure of about 1 Pa was investigated. The microstructure and strength of Ti_2AlC before and after healing at temperatures ranging from 1200 to 1400 ℃ for 1–4 h at a low oxygen partial pressure of about 1 Pa were characterized.

2 Experimental

2.1 Material preparation

Ti (average particle size = 48 μm, 99.5 wt% purity), Al (average particle size = 75 μm, 99.5 wt% purity), and TiC (average particle size = 48 μm, 99.5 wt% purity) powders were mixed in a plastic container for 10 h with a molar ratio of Ti : Al : TiC = 1 : 1.1 : 0.9. The mixture was hot-pressed in a graphite mold covered by BN at 1450 ℃ with 30 MPa for 1 h in the Ar atmosphere to synthesize Ti_2AlC samples [30].

The synthesized dense Ti_2AC samples were diamond-cut into bars with dimensions of 4 mm in width, 3 mm in thickness, and 36 mm in length. The rectangular bars were ground with SiC papers, and their tensile surfaces were polished to 0.25 μm by a diamond paste, and then cleaned in an ultrasonic bath with ethanol. Some polished bars were used to perform a three-point bending test, and others were used to introduce damages and to perform the healing test.

2.2 Damaging and crack healing

Microdamages were generated by indentation method. On the polished surface, a row of four indentations along the width in the middle of the long bar are generated using a diamond indenter in a Vickers hardness tester (TH700, Beijing TIME High Technology Ltd., China). The load was 30 kg, and the dwell time was 15 s. The damaged bars were heat-treated in a vacuum furnace at temperatures of 1200–1400 ℃ for 1–4 h. The residual pressure in the furnace was ~5 Pa, corresponding to a low oxygen partial pressure of about 1 Pa.

2. 3 Mechanical property measurement

To measure the initial strength, residual strength, and recovered strength, the three-point bending test was performed in a WDW-100E compression machine (Jinan Time Shijin Testing Machine Co., Ltd., China) by the initial polished bars, damaged bars, and healed bars. During the test, the polished surfaces and the damaged surfaces before and after healing were subjected to the tensile stress. The span size was 30 mm, and the crosshead speed was 0.5 mm/min. At least three bars were tested to achieve an average strength value.

2. 4 Characterization

The microstructures of the initial, damaged, and healed bars were characterized by a scanning electron microscope (ZEISS EVO 18, Carl Zeiss SMT, Germany) equipped with an energy-dispersive spectrometer (X-Max50, Bruker, Germany). The polished surfaces of the initial bars were etched by a mixed acid solution of HF and HNO_3, and then characterized with scanning electron microscopy (SEM)/energy-dispersive spectroscopy (EDS). The phase compositions of the samples before and after healing were identified by an X-ray diffractometer (XRD; D/Max 2200PC, Rigaku Co., Ltd., Japan) using Cu Kα radiation. The filling products in the healed zones were determined with XRD and EDS.

3 Results

The as-prepared sample mainly consists of Ti_2AlC, with a small amount of TiC as an impurity, evidenced by the XRD pattern (Fig. 1(a)). The etched surface demonstrates that the Ti_2AlC grains are plate-like, with sizes of ~45 μm in length and ~6 μm in thickness (Fig. 1(b)).

Figure 2 shows the flexural strengths for the original, damaged, and healed Ti_2AlC bars. The original Ti_2AlC material has a flexural strength of about 375 MPa. It should be noted that the healing of the original samples at 1400 ℃ for 2 h leads to an improved strength up to 421 MPa (Fig. 2(a)). The main reason will be explained in Section 4. Introducing damages by the indentation method causes a great decline of 50.4% in strength, from the initial strength of 375 to 186 MPa. The fractured samples after the bending test showed that the fracture propagation was through the four indentations in the damaged samples (the upper image in Fig. 2(b)).

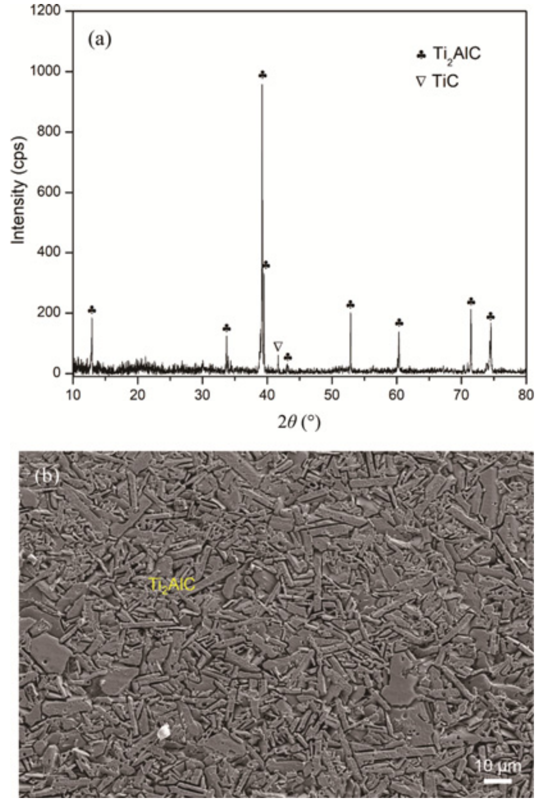

Fig. 1 Characterization of prepared Ti_2AlC sample: (a) XRD pattern and (b) SEM micrograph of etched surface.

After healing at different temperatures for various time at a low oxygen partial pressure of about 1 Pa, all the healed samples showed strength recovery. After healing at 1200 ℃ for 2 h, the strength recovered from 185 MPa for the residual strength to 340 MPa. However, the recovered strength is still lower than the initial strength. It should be noted that both healing temperature and time have a profound influence on the recovered strength. As the temperature increased to 1300 ℃, healing for 2 h leads to the recovered strength up to 371 MPa, almost twice the residual strength of 185 MPa, and close to the initial strength of 375 MPa.

After healing at 1400 ℃ for 1–4 h, all the healed samples exhibit the strength recovery exceeding the initial strength. For example, healing at 1400 ℃ for only 1 h leads to the strength recovering to 391 MPa. Healing for 2 h results in the recovered strength up to 405 MPa, close to 421 MPa for the original Ti_2AlC sample. After healing at 1400 ℃ for 4 h, a high recovered strength of 422 MPa was achieved, increased by 13% of the initial strength. However, prolonging time to 6 h at 1400 ℃ caused a decline in strength (not shown here).

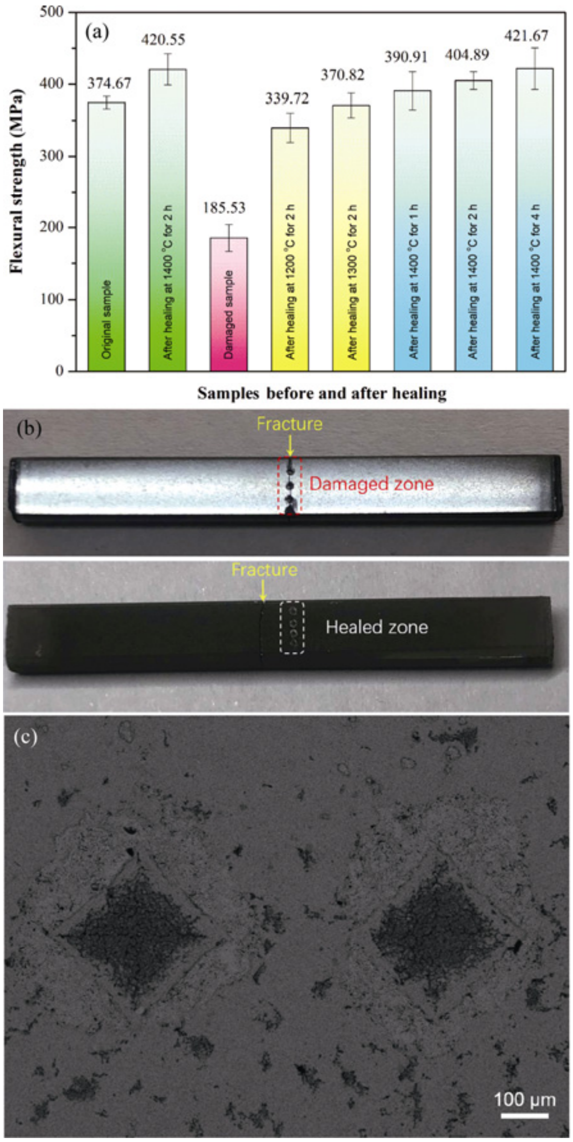

Fig. 2 (a) Flexural strengths for original, damaged, and healed Ti_2AlC samples. Error bars represent standard deviations. (b) Optical images of damaged bar (upper image) and the 1400 ℃–2 h-healed bar after fracture (lower image). (c) Back-scattered SEM image of healed zone on the 1400 ℃–2 h-healed bar.

Our previous work [1] demonstrated that the oxidation-induced crack healing of Ti_2AlC leads to the flexural strength returning from the initial strength (211 MPa) to 224 MPa after healing at 1200 ℃ for 2 h in air. It should be noted that the fracture path in the 1400 ℃–2 h-healed samples after the bending test was away from the healed zone, suggesting that the healed zone becomes stronger (the lower image in Fig. 2(b)). Such feature has also been observed in the Ti_2AlC and Cr_2AlC MAX materials after healing in the air [1,16]. Figure 2(c) presents another feature, in which the damaged zones around the indentations are completely covered, and the indentations are almost filled by some products. To identify the formed products and clarify the crack healing behavior of Ti_2AlC at a low oxygen partial pressure of about 1 Pa, the phase compositions and the microstructures of the healed samples were characterized with XRD and SEM/EDS.

After healing at temperatures of 1200–1400 ℃ for different times, the surfaces of the healed Ti_2AlC samples were characterized with XRD (Fig. 3). After healing at 1200 ℃ for 2 h, some Ti_2AlC peaks disappeared, and the main peak of (103) locating at 39.54° decreased greatly in intensity (Fig. 3(b)) as compared with that of the initial Ti_2AlC sample (Fig. 3(a)). In addition, new phases of Ti_3AlC_2, TiC, and Al_2O_3 were detected (Fig. 3(b)). After healing at 1300 ℃ for 2 h, the peak intensities of TiC became stronger, indicating that TiC is the predominant phase. However, Ti_2AlC, Ti_3AlC_2, and Al_2O_3 peaks still appeared. The above results indicate that the decomposition of Ti_2AlC into TiC_x (the value of x is theoretically 0.5) occurs at above 1200 ℃, and the appearance of Ti_3AlC_2 may be induced by a reaction between Ti_2AlC and TiC_x; the detailed information was analyzed in Section 4. After healing at 1400 ℃ for 2 h, only TiC peaks appeared, without Ti_3AlC_2 and Al_2O_3 peaks, indicating that the Ti_2AlC sample might have been completely transformed into TiC_x, or the surface of the healed sample may be covered by a TiC_x

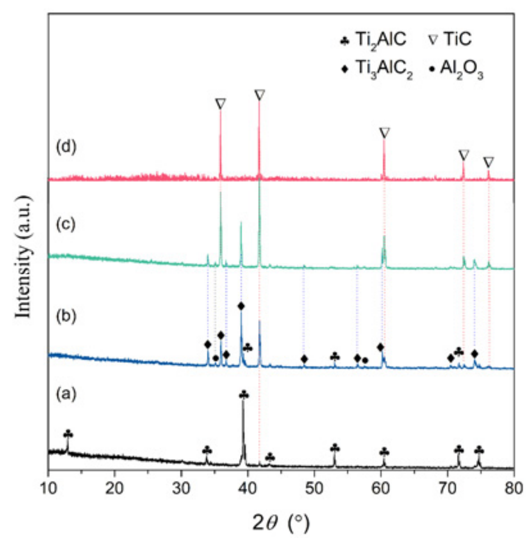

Fig. 3 XRD patterns of the Ti_2AlC samples: (a) before healing, and after healing for 2 h at (b) 1200 ℃, (c) 1300 ℃, and (d) 1400 ℃ at a low oxygen partial pressure of about 1 Pa.

layer with a thickness of large than 10 μm. The above supposition will be confirmed by the following cross-sectional SEM observations.

Cross-sectional SEM images of the damaged and healed Ti_2AlC samples are presented in Fig. 4. The fracture surface through the indentation shows a semielliptical damaged zone, where the larger Ti_2AlC grains are broken into small ones under a compressive load of 30 kg (Fig. 4(a)). Many micro cracks with transgranular and intergranular propagation paths were found under the indentation, as shown in the areas marked by "1" and "2" (Fig. 4(a)). These damages cause a drop of 50.4% in strength, as depicted in Fig. 2.

A low-magnification cross-sectional SEM micrograph of the 1200 ℃–2 h-healed Ti_2AlC reveals that the indentation was not completely filled by the products (the inset in Fig. 4(b)). A high-magnification SEM micrograph taken from the marked area in the inset clearly shows a dense layer covering the surface. The dense layer is mainly composed of fine TiC_x grains, identified by XRD and EDS. The TiC_x layer is about 1.4 μm in thickness (Fig. 4(b)). It should be noted that the micro cracks under the indentation completely disappeared, as compared with Fig. 4(a). With the temperature increasing, the TiC layer becomes thicker. The thickness of the TiC_x layer is about 5 μm in the 1300 ℃–2 h-healed Ti_2AlC (Fig. 4(c)), and about 20 μm in the 1400 ℃–2 h-healed Ti_2AlC (Fig. 4(d)). In addition, the thickness of the TiC_x layer is also influenced by the healing time. Healing at 1400 ℃

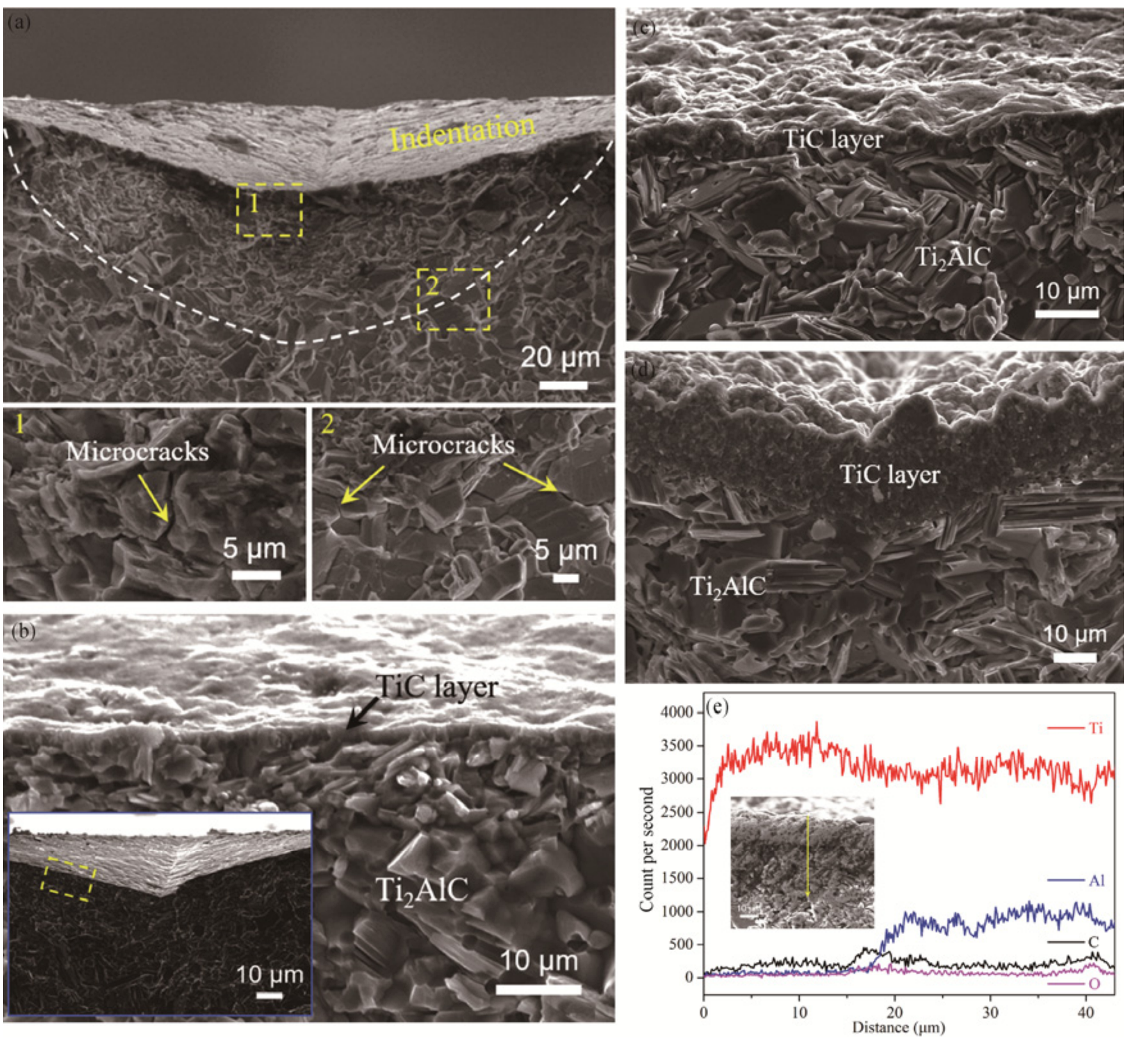

Fig. 4 Cross-sectional SEM micrographs: (a) damaged Ti_2AlC sample; and Ti_2AlC samples after healing for 2 h at (b) 1200 ℃, (c) 1300 ℃, and (d) 1400 ℃. (e) EDS line analysis along an arrow marked in inset for 1400 ℃–2 h-healed sample. Bottom panel in (a) shows two high-magnification SEM images taken from damaged zones marked by "1" and "2". Inset in (b) is a low-magnification SEM image, and dashed rectangle area is enlarged and shown in (b).

for 1–4 h leads to the layer thickness changing from 10 to 45 μm. The elemental distribution results showed that the surface layer mainly consists of Ti and C elements (59 at% Ti and 41 at% C), corresponding to TiC_x; the area below the TiC layer is comprised of Ti, Al, and C, indicating Ti_2AlC or Ti_3AlC_2 (Fig. 4(e)). Based on the XRD results, Ti_3AlC_2 appeared in the samples after healing at above 1200 ℃. Therefore, a mixture of Ti_2AlC and Ti_3AlC_2 may exist under the TiC_x layer.

Based on the above discussions, it can be concluded that Ti_2AlC can heal damages even at a low oxygen partial pressure of about 1 Pa; the main mechanism is that the formed TiC from the decomposition of Ti_2AlC fills the damages, leading to the strength recovery. For the Ti_2AlC MAX phase, it exhibits a new crack healing mechanism, i.e., decomposition-induced crack healing in the low oxygen partial pressure environments.

4 Discussion

To further investigate the microstructure of the healed zones under the indentations in Ti_2AlC at a low oxygen partial pressure of about 1 Pa, the polished fracture surface of the 1400 ℃–2 h-healed Ti_2AlC sample was characterized by SEM/EDS (Figs. 5 and 6). No exfoliation and crack in the area between the TiC layer and the damaged zones in the matrix were detected, indicating that the formed TiC layer bonds the matrix strongly (Fig. 5). For the original Ti_2AlC samples after healing at 1400 ℃ for 2 h, the surface defects such as scratches and holes should be filled by the formed TiC_x. For the damaged samples, the formed TiC_x fills all the damaged zones induced by indentation, contributing to the strength recovery. It can be found that small Al_2O_3 grains (black particles) fill the pores and micro cracks, explaining why the TiC layer is dense. The back-scattered SEM micrograph taken from the polished surface by removing the TiC layer about 15 μm in thickness from the surface clearly presents some small black particles in the pores or small cracks (Fig. 6(a)). The EDS mapping analysis shows the elemental distributions of Ti, Al, O, and C (Fig. 6(b)). The black particles are mainly composed of Al and O, being Al_2O_3.

Upon healing, the high temperature induces the decomposition reaction of Ti_2AlC. The decomposition preferentially occurs on the sample surface, especially

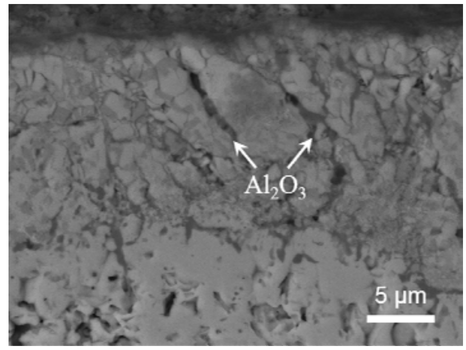

Fig. 5 Back-scattered SEM image of polished fracture surface of 1400 ℃–2 h-healed sample.

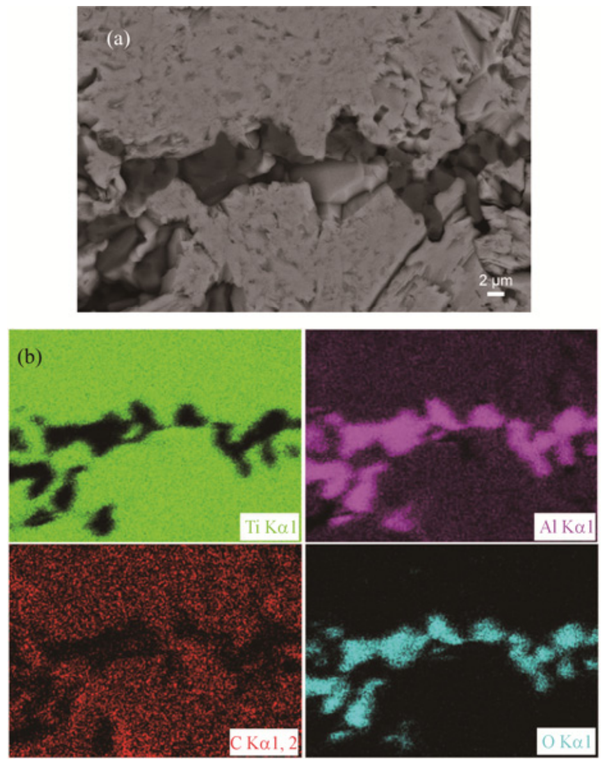

Fig. 6 (a) Back-scattered SEM image and (b) EDS mappings of polished surface of 1400 ℃–2 h-healed Ti_2AlC sample after removing TiC_x layer about 15 μm in thickness from surface.

in the damaged zones caused by the indentation due to the deformed Ti_2AlC grains with high strain energy. According to Reaction (1), Ti_2AlC decomposes into $TiC_{0.5}$ and Al. However, the content of C may be changed if Reaction (2) occurs [31]. Herein, TiC_x is denoted as the decomposed product.

$$Ti_2AlC(s) \rightarrow 2TiC_{0.5}(s) + Al(g) \quad (1)$$

$$Ti_2AlC(s) \rightarrow TiC(s) + Ti(g) + Al(g) \quad (2)$$

The TiC_x grains from the Ti_2AlC decomposition cover the surface and form a TiC_x layer, which becomes thicker with increasing temperature. The decomposition reaction of Ti_2AlC to form TiC_x results in a volume shrink. Therefore, many pores were detected in the TiC_x layer (Fig. 5), which act as diffusion channels for the evaporation of Al at a low oxygen partial pressure of about 1 Pa. When gaseous Al passes through the porous TiC_x layer, some Al atoms react with residual oxygen atoms in the system to form Al_2O_3, filling the pores and microcracks in the TiC_x layer. This explains the reason why small Al_2O_3 particles distribute in the TiC_x layer, as shown in Figs. 5 and 6.

According to the XRD results, the Ti_3AlC_2 peaks were detected after healing Ti_2AlC at 1200 and 1300 ℃ for 2 h (Fig. 3). The appearance of Ti_3AlC_2 may be due to a reaction between Ti_2AlC and TiC, as described by Reaction (3) [32]. However, the Ti_3AlC_2 phase finally decomposes into $TiC_{0.67}$ and Al as a gaseous phase at above 1200 ℃ in vacuum, as described by Reaction (4) [33]. It has been reported that the decomposition of Ti_3AlC_2 occurs at 1250 ℃ in an Ar or Ar–10 vol% CO atmosphere, resulting in the resultant products of $TiC_{0.67}$ and Al_2O_3 [34]. Wang and Zhou [35] found that Ti_3AlC_2 powder even decomposes at a temperature of as low as 600 ℃, and its decomposition rate is faster than that of the bulk counterpart in Ar [35].

$$Ti_2AlC(s) + TiC(s) \rightarrow Ti_3AlC_2(s) \quad (3)$$

$$Ti_3AlC_2(s) \rightarrow 3TiC_{0.67}(s) + Al(g) \quad (4)$$

As the temperature was 1400 ℃, the decomposition of both Ti_2AlC and Ti_3AlC_2 became severe, and the formed TiC_x as the main phase completely filled the micro-damages both under indentations and on the original surface. The Al_2O_3 content may be lower than the detection limit of the XRD. This explains why only TiC was detected in the 1400 ℃–2 h-healed sample by the XRD (Fig. 3).

It has been reported that the Ti_2AlC and Ti_3AlC_2 phases may decompose into TiC_x and two gaseous phases of Al and Ti at high temperatures [31]. In the present study, the residual pressure in the furnace was ~5 Pa, the vapor pressures of Al rise from 1.4 Pa at 1200 ℃ to 26 Pa at 1400 ℃, but the vapor pressures of Ti are over 3 orders of magnitude lower than those of Al at the same temperature (Table 1). The vapor pressures of Al and Ti are calculated according to $\log P_{Al}^0 = -16380T^{-1} - 0.66\log T + 12.3$ and $\log P_{Ti}^0 = -23200T^{-1} - 0.66\log T + 11.74$, respectively [36]. Therefore,

Table 1 Vapor pressure (P^0) of Ti and Al at different temperatures (T) (Unit: Pa)

T	1473 K	1573 K	1673 K
P_{Ti}^0	1.327×10^{-4}	1.014×10^{-3}	7.410×10^{-3}
P_{Al}^0	1.374	6.533	25.996

the decomposition of Ti_2AlC and Ti_3AlC_2 should be caused by the severe deintercalation of Al instead of Ti from their structures.

Once the relatively dense TiC_x layer forms on the surface of the Ti_2AlC sample, it acts as a barrier layer to retard the Al atomic migration from Ti_2AlC, and thus slows down the decomposition process.

The volume shrink caused by the decomposition of Ti_2AlC will generate a compressive stress in the TiC_x layer. In addition, the thermal expansion mismatch between the TiC_x layer and the Ti_2AlC matrix upon cooling down from the healing temperature also leads to the generation of the compressive stress on the healed surface. The coefficients of the thermal expansion for Ti_2AlC and TiC_x are 8.8×10^{-6} [14] and $(7.4–8.3)\times10^{-6}$ K^{-1} [14,37], respectively. The compressive stress generated in the TiC_x layer acts as a surface prestress to counteract the tensile stress applied to the surface of the Ti_2AlC material. In addition, it will be influenced by the thickness and microstructure of the TiC_x layer. This is the reason why the original and damaged Ti_2AlC samples after healing at 1400 ℃ have the recovered strength higher than the initial strength.

Based on the above discussions, it can be concluded that Ti_2AlC as a representative of the MAX phases can repair damages in vacuum or low oxygen partial pressure environments. The main mechanism is the decomposition-induced crack healing.

Up to now, two kinds of mechanisms have been confirmed for the self-healing of MAX phases at low oxygen partial pressures. Sn-precipitation-induced crack healing in Ti_2SnC is the main mechanism at a low oxygen partial pressure of 5 Pa [24]. The precipitation-induced crack healing mechanism is predominant in the MAX phases containing low-melting-point “A” elements such as Ga, Sn, In, and Pb, which have low migration energy. However, these MAX phases still keep the stable structural integrity after healing [24]. Decomposition-induced crack healing is the other mechanism confirmed in Ti_2AlC at temperatures above 1200 ℃ at low oxygen partial pressures. This mechanism may be effective in the Al- or Si-containing MAX phases (Ti_2AlC, Cr_2AlC, Ti_3AlC_2, and Ti_3SiC_2), which are triggered by the decomposition of the MAX on the surface into carbides such as TiC_x or $Cr_{23}C_6$ [38] at high temperatures.

5 Conclusions

The crack healing behavior of Ti_2AlC was firstly investigated in the temperature range of 1200–1400 ℃ for 1–4 h at a low oxygen partial pressure of about 1 Pa. The healing tests demonstrated that Ti_2AlC has the ability to heal damages even under the low oxygen partial pressure condition. Healing at 1300 ℃ for 2 h leads the strength recovery to 371 MPa, close to the initial strength of 375 MPa. After healing at 1400 ℃, all the healed samples have the strength recovery exceeding the initial strength. A high recovered strength of 422 MPa was achieved after healing at 1400 ℃ for 4 h, increased by 13% of the initial strength. Decomposition-induced crack healing as a new healing mechanism in the Ti_2AlC MAX phase was confirmed upon healing in the low oxygen partial pressure environment. The damages were healed by the formed TiC_x from the decomposition of Ti_2AlC on the surface. In addition, some Al atoms from Ti_2AlC reacted with residual O in the system to form Al_2O_3. The small Al_2O_3 grains fill the pores in the TiC_x layer, thereby making the healed zones relatively dense. The healing ability of Ti_2AlC in low oxygen partial pressure environments widens the potential applications of MAX phases in different environments.

Acknowledgements

This work was supported by the National Natural Science Foundation of China (No. 52275171) and the Pre-Research Program in National 14th Five-Year Plan (No. 80923010304).

Declaration of competing interest

The authors have no competing interests to declare that are relevant to the content of this article.

References

[1] Li SB, Song GM, Kwakernaak K, *et al*. Multiple crack healing of a Ti_2AlC ceramic. *J Eur Ceram Soc* 2012, **32**: 1813–1820.

[2] Van der Zwaag S, van Dijk NH, Jonkers HM, *et al*. Self-healing behaviour in man-made engineering materials: Bioinspired but taking into account their intrinsic character. *Philos Trans Roy Soc A Math Phys Eng Sci* 2009, **367**: 1689–1704.

[3] Fratzl P. Self-healing materials: An alternative approach to 20 centuries of materials science. *J Chem Int* 2014, **30**: 20–21.

[4] Lu XG, Li SB, Zhang WW, *et al*. Crack healing behavior of a MAB phase: MoAlB. *J Eur Ceram Soc* 2019, **39**: 4023–4028.

[5] Lange FF, Gupta TK. Crack healing by heat treatment. *J Am Ceram Soc* 1970, **53**: 54–55.

[6] Roberts JTA, Wrona BJ. Crack healing in UO_2. *J Am Ceram Soc* 1973, **56**: 297–299.

[7] Gupta TK. Crack healing and strengthening of thermally shocked alumina. *J Am Ceram Soc* 1976, **59**: 259–262.

[8] Lange FF. Healing of surface cracks in SiC by oxidation. *J Am Ceram Soc* 1970, **53**: 290.

[9] Easler TE, Bradt RC, Tressler RE. Effects of oxidation and oxidation under load on strength distributions of Si_3N_4. *J Am Ceram Soc* 1982, **65**: 317–320.

[10] Zhang YH, Edwards L, Plumbridge WJ. Crack healing in a silicon nitride ceramic. *J Am Ceram Soc* 1998, **81**: 1861–1868.

[11] Takahashi K, Yokouchi M, Lee SK, *et al*. Crack-healing behavior of Al_2O_3 toughened by SiC whiskers. *J Am Ceram Soc* 2003, **86**: 2143–2147.

[12] Greil P. Generic principles of crack-healing ceramics. *J Adv Ceram* 2012, **1**: 249–267.

[13] Zhou AG, Liu Y, Li SB, *et al*. From structural ceramics to 2D materials with multi-applications: A review on the development from MAX phases to MXenes. *J Adv Ceram* 2021, **10**: 1194–1242.

[14] Barsoum MW. The $M_{N+1}AX_N$ phases: A new class of solids. *Prog Solid State Chem* 2000, **28**: 201–281.

[15] Song GM, Pei YT, Sloof WG, *et al*. Oxidation-induced crack healing in Ti_3AlC_2 ceramics. *Scripta Mater* 2008, **58**: 13–16.

[16] Li SB, Xiao LO, Song GM, *et al*. Oxidation and crack healing behavior of a fine-grained Cr_2AlC ceramic. *J Am Ceram Soc* 2013, **96**: 892–899.

[17] Li SB, Bei GP, Chen XD, *et al*. Crack healing induced electrical and mechanical properties recovery in a Ti_2SnC ceramic. *J Eur Ceram Soc* 2016, **36**: 25–32.

[18] Bei GP, Pedimonte BJ, Fey T, *et al*. Oxidation behavior of MAX phase $Ti_2Al_{(1-x)}Sn_xC$ solid solution. *J Am Ceram Soc* 2013, **96**: 1359–1362.

[19] Yang HJ, Pei YT, Rao JC, *et al*. Self-healing performance of Ti_2AlC ceramic. *J Mater Chem* 2012, **22**: 8304–8313.

[20] Burk S, Gorr B, Christ HJ. High temperature oxidation of Mo–Si–B alloys: Effect of low and very low oxygen partial pressures. *Acta Mater* 2010, **58**: 6154–6165.

[21] Jacobson NS. Corrosion of silicon-based ceramics in combustion environments. *J Am Ceram Soc* 1993, **76**: 3–28.

[22] Zhang XH, Xu L, Du SY, *et al*. Preoxidation and crack-healing behavior of ZrB_2–SiC ceramic composite. *J Am Ceram Soc* 2008, **91**: 4068–4073.

[23] Li N, Hu P, Zhang XH, *et al*. Effects of oxygen partial pressure and atomic oxygen on the microstructure of oxide scale of ZrB_2–SiC composites at 1500 ℃. *Corros Sci* 2013, **73**: 44–53.

[24] Li SB, Zhang LQ, Yu WB, *et al*. Precipitation induced crack healing in a Ti_2SnC ceramic in vacuum. *Ceram Int* 2017, **43**: 6963–6966.

[25] Song GM, Schnabel V, Kwakernaak C, *et al*. High temperature oxidation behaviour of Ti_2AlC ceramic at 1200 ℃. *Mater High Temp* 2012, **29**: 205–209.

[26] Wang XH, Zhou YC. High-temperature oxidation behavior of Ti_2AlC in air. *Oxid Met* 2003, **59**: 303–320.

[27] Rao JC, Pei YT, Yang HJ, *et al*. TEM study of the initial oxide scales of Ti_2AlC. *Acta Mater* 2011, **59**: 5216–5223.

[28] Song GM, Li SB, Zhao CX, *et al*. Ultra-high temperature ablation behavior of Ti_2AlC ceramics under an oxyacetylene flame. *J Eur Ceram Soc* 2011, **31**: 855–862.

[29] Bai YL, Kong FY, He XD, *et al*. Thermal shock behavior of Ti_2AlC from 200 ℃ to 1400 ℃. *J Am Ceram Soc* 2017, **100**: 4190–4198.

[30] Cai LP, Huang ZY, Hu WQ, *et al*. The synthesis and mechanical properties of high pure $Ti_2Al(Sn)C$ solid solution. *Int J Appl Ceram Technol* 2018, **15**: 1212–1221.

[31] Pang WK, Low IM, O'Connor BH, *et al*. Comparison of thermal stability in MAX 211 and 312 phases. *J Phys Conf Ser* 2010, **251**: 012025.

[32] Kisi EH, Wu ED, Zobec JS, *et al*. Inter-conversion of $M_{n+1}AX_n$ phases in the Ti–Al–C system. *J Am Ceram Soc* 2007, **90**: 1912–1916.

[33] Pang WK, Low IM, Sun ZM. *In situ* high-temperature diffraction study of the thermal dissociation of Ti_3AlC_2 in vacuum. *J Am Ceram Soc* 2010, **93**: 2871–2876.

[34] Gai JL, Chen JX, Li MS. Thermal stability of Ti_3AlC_2 in Ar–10vol.%CO atmosphere. *J Eur Ceram Soc* 2016, **36**: 2837–2841.

[35] Wang XH, Zhou YC. Stability and selective oxidation of aluminum in nano-laminate Ti_3AlC_2 upon heating in argon. *Chem Mater* 2003, **15**: 3716–3720.

[36] Su YQ, Guo JJ, Jia J, *et al*. The evaporation of alloying element during vacuum melting of TiAl intermetallics. *Foundry* 1999: 1–4. (in Chinese)

[37] Houska CR. Thermal expansion of certain group IV and group V carbides at high temperatures. *J Am Ceram Soc* 1964, **47**: 310–311.

[38] Xiao LO, Li SB, Song GM, *et al*. Synthesis and thermal stability of Cr_2AlC. *J Eur Ceram Soc* 2011, **31**: 1497–1502.